

Breakthrough in Mars Balloon Technology

V.V.Kerzhanovich⁽¹⁾, J.Cutts⁽¹⁾, H.Cooper⁽¹⁾, J.Hall⁽¹⁾, B.McDonald⁽¹⁾, M.Pauken⁽¹⁾, C.White⁽¹⁾,
A.Yavrouin⁽¹⁾, A.Castano⁽¹⁾, H.Cathey⁽²⁾, D.Fairbrother⁽²⁾, S.Smith⁽²⁾, C.Shreves⁽²⁾, T.Lachenmeier⁽³⁾,
E.Rainwater⁽⁴⁾ and M.Smith⁽⁴⁾

ABSTRACT

At the end of 1997, JPL initiated a the Mars Balloon Validation Program (MABVAP) to develop and validate the technology needed for a Mars balloon mission. The program drew on experiences of the previous Mars Balloon development efforts – Russian-French Mars Aerostat led by the French space agency CNES. Several NASA Centers also contributed to various stages of the test program – Langley, Ames, Lewis and Dryden. In 1999, NASA Goddard Space Flight Center, which had collaborated with JPL on earlier Mars balloon concepts prior to 1997, became a partner in MABVAP. The main focus of MABVAP was to develop and to test a viable concept for the Martian balloon that could be implemented on the small-scale dedicated or piggy-back mission.

The MABVAP was based on several principles: design compatibility with a small Mars micromission with scientifically meaningful payload; evolvability to long-duration flights and to larger sizes; and fabrication from known and proven materials. A comprehensive step-by-step test program was planned involving tests in a Mars-like environment for validation. Models simulating deployment and inflation at Mars would be validated by these Earth based tests. The program was designed to be flexible enough to be modified based on results of each step.

The major phases of the program were:

- baseline concept definition that included preliminary tests of sub-scale balloons in wind tunnel, vacuum chamber and free drop tests,
- ground and flight tests of sub-scale and full-scale balloons at hangars, vacuum chamber, and in troposphere, pull-tests of full-scale balloons,
- stratospheric deployment/inflation tests in the Martian-like environment. A

number of models have been developed to better understand test results and make design changes.

Two major features – relatively small balloon and bottom inflation – contributed to ultimate success of the development. Two balloon designs were tested – 10-m spherical Mylar balloon and 500 m³ polyethylene pumpkin balloon. After meeting milestones in the first year of the program it experienced funding shortfalls which meant that modeling and simulation work was reduced and the costs of conducting flight tests had to radically reduced impacting reliability and to stretch out the duration of the program by an additional two years. This had its greatest impact on the stratospheric flight test program which the French experience had indicated to be the most challenging stage of development. Of nine stratospheric tests, four failed because of tow-balloon/launch failures or failures not related to the test balloon itself. The five remaining tests brought meaningful results – four with spherical balloons and one with a pumpkin balloon. In two of the spherical balloon tests, the balloon envelope ruptured on deployment. Analysis, modification of design and laboratory tests that followed these failures resulted very recently in two successful stratospheric tests – one with spherical and another – with pumpkin balloon.

Though there is still a number of design details that should be tuned before the real mission, we believe that feasibility of the Mars Balloon concept has been proven.

INTRODUCTION

Balloons may become powerful tools in the future exploration of Mars. Large surface coverage, access to rugged terrain and stable attitude during the flight are clear advantages of them.

(1) Jet Propulsion Laboratory, California
Institute of Technology, Pasadena, CA
(2) Wallops Flight Facility, Goddard Space
Flight Center
(3) CSST, Inc. Hillboro, OR

If so, then why no balloons flew on Mars yet? The main problem is Mars environment which probably is the most challenging among all planets with atmospheres.

First, very low the density of the Martian atmosphere that is equivalent to the stratosphere of Earth above 35 km requires large balloons to carry even light payloads.

Second, the daily surface temperature variations on Mars that determine balloon temperature may exceed 50%. As well known, it results in necessity of respective ballast drops for zero-pressure balloons and to ability to withstand superpressure almost equal to ambient pressure for superpressure balloons. The result is that zero-pressure balloons may survive only one day that practically excludes their usage for meaningful science missions (if not in the polar areas during polar day or polar night).

Third, deployment and inflation during parachute descent is the only practical way of balloon insertion on Mars. Aerial deployment and inflation has its own problems: balloon should be densely packed and stored during the interplanetary flight, it should survive deployment loads, it should be inflated safely in a few minutes. There was no relevant experience of deployment large thin-film inflatable structures in the stratosphere. The study of this process, design work and tests should precede to any Martian balloon missions. Development of technology of the aerial deployment and inflation of thin-film balloon in Martian environment was one of strategic objectives of MABVAP.

BACKGROUND

The first practical concept for a balloon mission in the atmosphere of Mars was initiated in 1986 by French and Soviet researchers. The concept was based on the success of the first planetary balloon mission – the Venus VEGA Balloons of 1985. The Planetary Society participated in this program with Soviets and French, and developed the concept of the snake or guiderope - which enabled the balloon to tolerate diurnal descents to the surface as the balloon cooled at night and permitted a mission duration of about 10 days as well as in situ surface data. A number of studies and tests have been performed that clarified various aspects of the Mars Aerostat performance.

However the most critical phase – aerial deployment and inflation of a thin-film balloon in the Martian-like environment has not been demonstrated (1). Due to budget problems the Russian-French development was terminated in 1995.

The later concepts – the Mars Aerial Platform (MAP) proposal to the NASA Discovery program in 1994 (2) and the Mars Aerobot/Balloon Study (MABS), carried out for NASA in 1996 (3), focused on the use of superpressure balloon with its potential for long-duration mission of up to 90 days. The MABS study involved collaboration with the NASA stratospheric balloon research program at NASA's Wallops Flight Facility (WFF) and is a fine example of spin-off from space programs played a role in the formulation of NASA's Earth's Ultra-Long Duration Balloon (ULDB) project by WFF. But again the deployment and inflation of the balloon was not addressed in detail.

MARS AEROBOT VALIDATION PROGRAM

The Mars Balloon Validation Program (MABVAP) was initiated in August 1997 and was conceived as a low-cost earth-based program to be completed prior to carrying out a real Mars balloon mission. There are three major components to MABVAP: validation of aerial deployment and inflation, superpressure balloon design and development of new simulation tools. Though the primary emphasis was on the first – the most critical part, significant progress is now being extended to the other two areas.

Mars Balloon program benefited greatly by WFF development of pumpkin balloon that became a core of the NASA ULDB Program. Collaboration of WFF and JPL in frame of the NASA Cross-Enterprise Technology Program led to study, design and fabrication of pumpkin balloon that could be suitable for the Mars application.

Two stratospheric test failures stimulated development of more detailed models of balloon structure and deployment process. The speed of progress in the MABVAP has been and continues to be limited by budget constraints.

Approach: Our approach to validation of deployment and inflation of a Mars balloon consisted of three phases which became progressively more costly to implement. This approach was devised after extensive consultation with the balloon community and in particular with the CNES team that developed and tested the Mars Aerostat:

Phase 1 – Concept Development; In this first phase, the intent was to explore configuration options, to test the concept at small scale in the laboratory, wind tunnel, vacuum chamber and in free drop tests and to establish the design space by using similarity methods.

Phase 2 – Prototype flight system development and pre-flight qualification: In this phase, functionally performing systems were built, ground and flight tests of sub-scale and full-scale balloons at hangars, vacuum chamber, and in troposphere, pull-tests of full-scale balloons have been conducted. This step confirmed the design choices made on the smaller scale and built confidence in the performance in the Martian-like environment.

Phase 3 – Stratospheric validation: The goal of this phase was to demonstrate and validate the design approach used in the closest approximation to the environment of Mars– the Earth’s stratosphere. Our philosophy was to test full-scale balloons instead of trying to extrapolate results of smaller balloon tests because absence of credible models could make this extrapolation unconvincing. This was the most critical and challenging stage where we encountered drawbacks as in test themselves as in launch operations. Each test was carefully analyzed, modifications been made, additional laboratory and hangar tests performed, more detailed models developed and the test was repeated. The stratospheric tests proved viability of the concept that was validated without major changes.

We drew on the experience of other projects. Many individuals and organizations supported MABVAP: French CNES (J.Blamont, A.Vargas, J.Evrard) shared results of Mars Aerostat project, participated in our tests and performed deployment simulations for us, South-West Research Institute (B.Perry) described the approach of OBJS project, NASA Centers Langley (R.Whipple, M.Fremaux), Dryden (J.Baer-Riedhard, J.Bauer, M.Rivas), Glenn

(J.Carek), Ames (L.Lewis, D.Ferguson) provided critical test support, discussions with J.Rand (Winzen Engineering) were important in the concept design and test definition, N.Kjomi (University of Wisconsin) helped to polish with launch procedures. We enjoyed the support of the FAA, FCC and local authorities of County of Hawaii and BLM for the flight tests.

MARS BALLOON DEPLOYMENT AND INFLATION CONCEPT

The concept and results of first two stages were described elsewhere [X] and will be only briefly summarized here.

The concept of Mars balloon mission is shown in Fig.1.

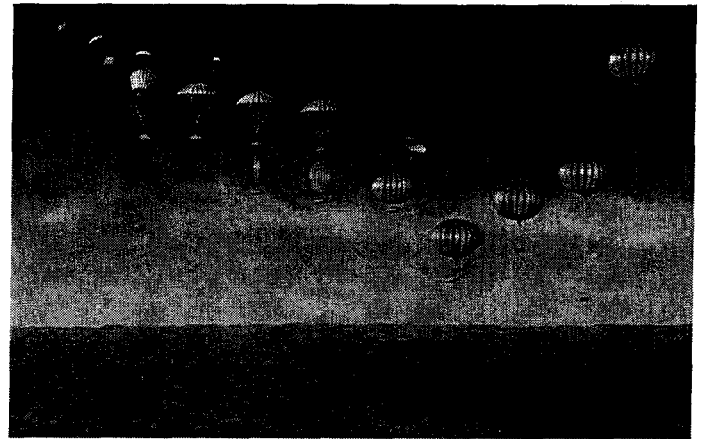


Fig.1. Aerial deployment and inflation concept (pumpkin balloon shown)

The balloon with all associated systems is packed inside aeroshell. After entering into the atmosphere the aftshell and the heatshield separate and the parachute deploys. Few seconds after reaching the terminal velocity the balloon container opens and the balloon deploys with the suspended inflation system and payload. At some moment after start of the inflation the parachute releases, the balloon with the inflation system continue to descend. The inflation system is released when the inflation process is completed and the balloon and the parachute reach sufficient separation; the balloon starts to ascend to the float altitude.

Since the density of the Martian atmosphere is so low, the deployment starts at 7-10 km above the average surface; the separation of the inflation system – the lowest point - should be 1-2 km above the real surface. The whole process should be completed in 200-300 sec

The bottom inflation concept was selected since it may be more mass efficient, it is less subject to aerodynamic instabilities and there is less risk of damage of the balloon with the descending parachute after their separation.

There are many problems associated with each stage of the deployment/inflation process. The most critical are: mitigation of deployment shocks; possible twisting of the balloon; possible aerodynamic instabilities; avoiding if possible a need for reefing the balloon; propagation of the helium bubble to the top of the balloon when inflated from the bottom; possible damage of the balloon during helium inflation with a rapidly expanding helium (expansion rate $\sim 22 \text{ m}^3/\text{s}$); residual gas evacuation; compact packaging of the spherical balloon; balloon design for the airborne deployment

Both analytical and test approaches were used to study some of the problems.

Baseline test configuration.

Balloon. Mission design studies based on recent JPL experience with DS-2 Mars Microprobes showed that 10-m spherical balloon can carry scientifically meaningful payload of 1-2 kg of mass; this payload would be adequate for the first balloon-based Mars mission (at this time spherical design was also a baseline for the ULDB program). It implied also that the areal density of balloon material should not exceed 10-12 g/m². Following results of earlier CNES studies we adopted 8-12 mk Mylar C film as a baseline material for fabrication of balloon prototypes.

Three other parallel efforts were initiated to improve material and balloon design: Foster-Miller Inc SBIR program to develop PBO film with uniformity acceptable for Mars balloon applications, Winzen Engineering SBIR program to develop and test other films and light-weight composites, GSSL SBIR program to develop balloon with embedded net. In course of development of the ULDB program WFF adopted the pumpkin design. The latest progress and tests allowed to adopt the pumpkin as an

alternative option for Mars balloon prototype (see further).

Mitigating balloon envelope stresses during deployment: If no restraint mechanisms (such as a braking wheel) are used, the balloon starts a free fall when it deploys from its container. Abrupt deceleration of the inflation system suspended from the bottom of the balloon by the balloon envelope produces a shock load at the end of the deployment that would destroy the envelope.

Several approaches to shock mitigation were investigated. Finally, two ripstitches (upper - between balloon and parachute, lower between balloon and inflation module) were adopted as shock absorbers (four ripstitches used in our latest system). Ripstitches are more reliable though less precise than other devices considered.

To reduce risk of damaging of the envelope we adopted a new “fold-and-roll” method of packaging of the balloon when the balloon unrolls during the deployment. The final shock occurs closer to the middle of the balloon where it is taken by much more amount of film than near the fittings.

Bottom inflation. Wind tunnel tests were performed in the vertical wind tunnel at NASA Langley Research Center. A 2-m spherical Mylar balloon with attached 1.5-m diameter parachute were subjected to the air velocities from 2.5 to 7 m/s that corresponds to dynamic pressures from ~ 4 to 29 Pa (it covers all feasible range for balloon deployment). The typical shape of the balloon during the tests is shown on Figure 2.

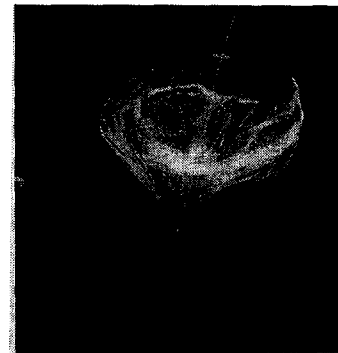


Fig 2. Balloon in the LaRC Vertical Wind Tunnel

These tests as well as a number of free drop tests of subscale balloon under parachute and with an appropriate payload demonstrated highly stable behavior of the system when balloon is inflated for less than 50-60% of its volume even in presence of pronounced spinnakering. Oscillations with the Struhal frequency gradually develop when balloon is inflated for more than 60% and falls without parachute. Parachute significantly decreases amplitude of these oscillations.

Inflation system and static inflation tests. The inflation system was designed to deliver helium with the maximum rate ~20 g/sec. It included one or two helium tanks, two pyrovalves, pressure and temperature transducers, isolation and relief valves. The flexible hose connected system with the diffuser within the balloon.

The maximum capacity of the inflation system is 0.9 kg of helium at 300 atmospheres (in stratospheric tests only one tank with 450 g of helium was used). The inflation system was adjusted to complete inflation in 60-100 sec. A flexible fabric diffuser or "windsock" made of nylon with ~ 50% porosity was attached to the output of the metal diffuser. Several inflation tests were conducted in a low pressure chambers at JPL and the GRC Plumbrook facility in order to optimize the design and verify balloon inflation in static. Fig.3 shows inflation of full-scale balloon in GRC. Only 450 g of helium was needed to fill the 10 m diameter (523 m³ balloon at 5 mb and ambient temperature of near 290K. Inflation of balloon was completed successfully in approximately 30 seconds.



Figure 3. Inflation of 10-m Mylar balloon in NASA Glenn Research Center

Static deployment tests. Several static deployment tests were performed at JPL and at the GSSL hangar in Tillamook, Oregon. Term "static" means that the packed balloon was suspended under a fixed structure (crane or hangar structure) and hence did not simulated completely in-flight process. Two 10-m Mylar balloons – one made of 12 μ film another of 8 μ film – were deployed three times each with attached payload from 25 to 35 kg. All tests were successful; the inspection did not find any damages in the balloons.

Success in all ground tests allowed proceeding to the critical phase of flight tests. Schematic of stratospheric flight tests – ultimate goal of the program – is shown in Fig.4.

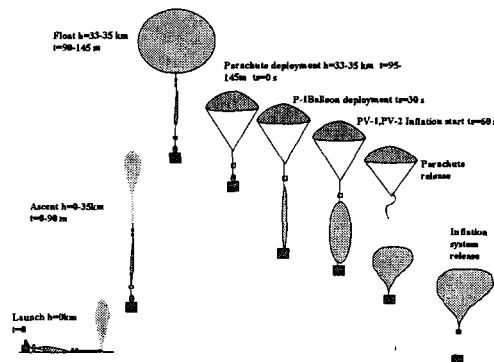


Figure 4. Diagram of stratospheric tests

Comparison of Fig.3 and Fig.4 shows that the stratospheric test reproduces all phases of the real mission starting parachute descent. Earlier phases - entry and parachute deployment – are parts of a standard entry sequence and were demonstrated successfully in the previous programs (Viking, Mars Pathfinder).

Main test article – deployment module (DM) typically included balloon container with packed balloon, inflation system, command/data system, up-looking camera with TV transmitter, flight controller, set of sensors (accelerometers, load cells, pressure and temperature in elements of inflation system etc) and radiosonde. Sensors and other elements of avionics were modified for a new test based on previous results.

Ripstitches and carefully adjusted Kevlar tethers and bridles controlled deployment sequence.. The DM was suspended under the parachute

attached to the stratospheric tow-balloon. Set of pyro guillotines and pyrovalves used to initiate subsequent steps in deployment and inflation (D&I) process. A separate unit with down-looking camera and transmitter attached between the parachute and DM.

Tropospheric flight tests. Three tropospheric flight tests were conducted to adjust to validate performance of the flight train components. In the last of them (LAT-3) 3-m spherical Mylar balloon made of 12m film was successfully deployed and inflated (Figure 5). This test provided an opportunity to validate the use of the bottom inflation system and thin-film balloons for missions to bodies with much denser atmospheres than Mars – specifically Venus and Titan.



Figure .5. LAT-3 Deployment and inflation of 3-m Mylar balloon

EARLIER STRATOSPHERIC TESTS

For the stratospheric tests, some design changes were made: flexible fabric bag replaced the heavy solid balloon container; a real time video system replaced the camcorders; the flight avionics was qualified in a thermo vacuum chamber. Prior to each test the balloon was packed into bag and placed in the vacuum

chamber to remove residual gas. Only one gas tank was used to simulate Martian loads better. Disk parachute 7.2 m diameter used in the first three attempts, 10.8-m cruciform – in the others.

Six flight test attempts were conducted in 1998-2001. Three of them failed at the ground due to failures of tow-balloon or during launch. The first attempt was made from the boat in the Gulf of Mexico. All subsequent tests were launched from a lava terrain near the South Point of Big Island of Hawaii. All were hand launches and did not use any special launch equipment. Summary of the test results is given in Table 1.

Table 1

Test	Date	Objective	Modification	Result
STRA-1	Oct98	D&I 10-m Mylar balloon System test		Tow-balloon failed before launch
STRA-2	Jan99	D&I 10-m Mylar balloon at 35km	New DM New location	Tow-balloon failed during inflation
STRA-2A	Mar99	D&I 10-m Mylar balloon at 35km System test	Launch simulation New launch procedures	Successful launch Successful balloon deployment Balloon failure after 52 sec of inflation
STRA-3	Nov99	D&I 10-m Mylar balloon at 35km System test	Low-temperature tapes in balloon New DM New parachute Improved ground station	Tow-balloon destruction during the launch
STRA-4	Feb00	Repeat test STRA-3	Improvements in launch procedures	Successful launch Balloon failed near bottom fitting at deployment
STRA-5	Feb01	Repeat test STRA-4	Modified balloon fittings Reinforced balloon doublers Improved balloon quality control	Successful launch Balloon failed near upper fitting at deployment

The successful STRA-2A test used the same 12m balloon that previously passed inflation test at GRC and deployment test at GSSL. Though deployed successfully it failed during inflation when almost 80% of gas was already inserted. Balloon failure during inflation was attributed to

use of pressure-activated tapes in the balloon not rated for cold temperatures especially during balloon inflation.

Two other tests successfully launched (STRA-4 and STRA-5) failed during deployment in spite of reinforcement in the balloon and precautions in flight train preparations. These failures stimulated review of the concept, procedures and stimulated new attempt of detailed simulation of balloon deployment process as well as new series of ground tests.

IN-DEPTH SIMULATION OF DEPLOYMENT PROCESS

Simulation models of the balloon and of the deployment process were created for the purpose of estimating the design margin of the flight system. Other benefits of the models include a greater understanding of the deployment process, the ability to predict lengths of ripstitch that would be needed for any specific deployment configuration, and assistance in designing hangar-based deployment experiments.

A key parameter in the deployment forces is the velocity difference between the top and bottom of the balloon during the snap event. Forces from the parachute aerodynamics and flight train masses determine the kinematics of the upper half of the balloon, while gravitational acceleration and comparatively small drag forces act on the lower half. The snap occurs when the distance between the balloon upper fitting and the lower fitting is equal to the length of the balloon. A lumped mass rigid body model that includes the variable mass of the spooled balloon and the variable mass of the upper and lower halves as deployment progresses was used to compute the separation velocity (ΔV) at the snap instant.

Once the separation velocities were estimated, they could be used as kinematic initial conditions for a highly discretized lumped spring-mass model of the balloon. Other flight train elements (parachute, cameras, pyro controls, telemetry transmitters, etc) were included as discrete rigid masses connected by stiff springs. The application of different velocities to the upper and lower regions of the fully deployed balloon simulates the snap event. Balloon stiffness is a nonlinear (stiffening) function that was determined from static pull tests in the lab. In addition to the separation velocity, the point

where the two different velocities are assumed to meet is another critical parameter for determining internal balloon forces. Based on reviewing video documentation of many hangar drop tests and analysis work, this point is known to fall somewhere in the lower half of the balloon. Figure 6 illustrates the axial force variation with both position and time in the balloon. Note the reflection of the force wave from the lower end fitting of the balloon.

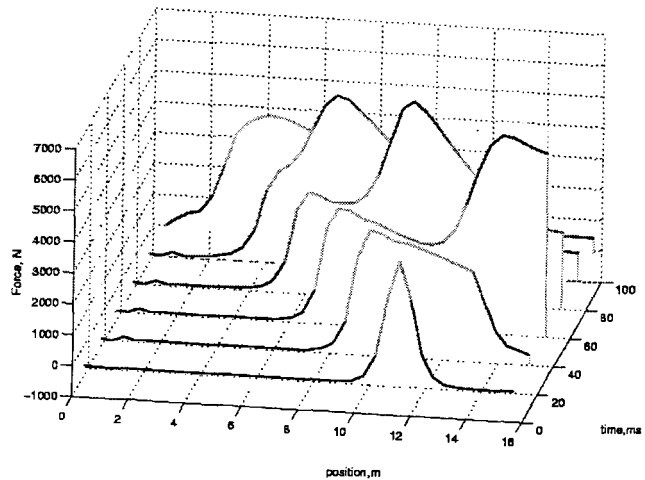


Figure 6. Evolution of axial force in balloon during deployment snap

The spring mass model, being a great simplification, is capable of capturing only the essential deployment mechanics, in particular the resultant internal axial force in all elements of the flight train, the kinematic responses of the lumped masses, and the amount of energy dissipated and length torn through the ripstitch. The actual uninflated balloon structure possesses a highly nonlinear response, both in materials and geometrically.

From the geometrical standpoint alone, the balloon has an infinite number of underformed equilibrium positions, and a great many equilibria when pulled with an axial load. Many of the material properties of the Mylar, adhesives, tapes, and composite fabrics are variable and uncertain, and likely depend on temperature, humidity, and strain rate. The possible presence of initial flaws or pinholes in the Mylar material complicates the analysis of design margin. Nevertheless, a finite element model was created and analyzed using the LS-

DYNA-3D computer program. The goal was to identify the critically stressed regions and to have a platform for evaluating potential balloon design changes.

The nonlinear analysis was initiated from the 1/8th symmetry model of the nominal design geometry, as shown in Figure 7. With the nodes

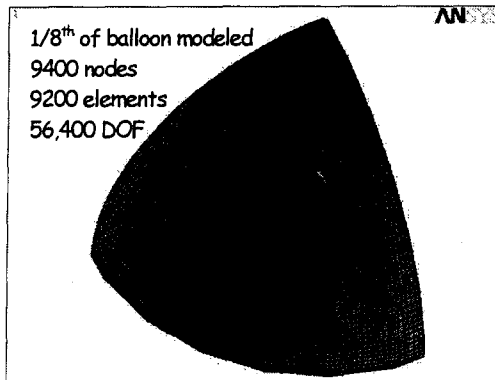


Figure 7. Undeformed finite element mesh of balloon model

along the equator restrained in the pole-to-pole direction, the apex was slowly pulled with a small force until the balloon achieved some stiffness in the axial direction. Stresses developed in the film as the load was increased. The final load of 4000N was based on a static approximation for the snap load as predicted from the deployment model described above. The final configuration predicted by the model is shown in Figure 8. At 4000N significant buckling has taken place in the cap stiffener around the end fitting, with corresponding pleats or folds in the balloon skin extending outwards to the equator. Peak stresses were found in the doubled up film material adjacent to the ring stiffener, and again in the clear 12 micron thick film adjacent to the largest doubler.

The prediction of the design margin during deployment remains a challenge, due to three issues: (1) the lack of a clearly defined failure mode for the balloon (strain rate effects, initial flaws, overstressing, or other); (2) uncertainties in material properties, and (3) the inherent variability in deployment forces that has been observed through experiments. Investigation is continuing on these topics, and models are being considered for the inflation aspect of the deployment.

DYNAMIC DEPLOYMENT TESTS

Three new rounds of deployment tests were conducted in the hangar of the NASA Ames Research Center in July 01- April 02. Their objective was to simulate stratospheric deployment, acquire detailed data on forces and kinematics and dynamics of deployment that can be compared to the models, to define balloon integrity margins and to test concept of deployment with external load line.

The idea was to subject balloon to deployment with progressively faster speed and to bring balloon to failure. A system of bungees was used to accelerate upper part of the balloon and in some tests – payload. Test configuration is shown in Figure 9.

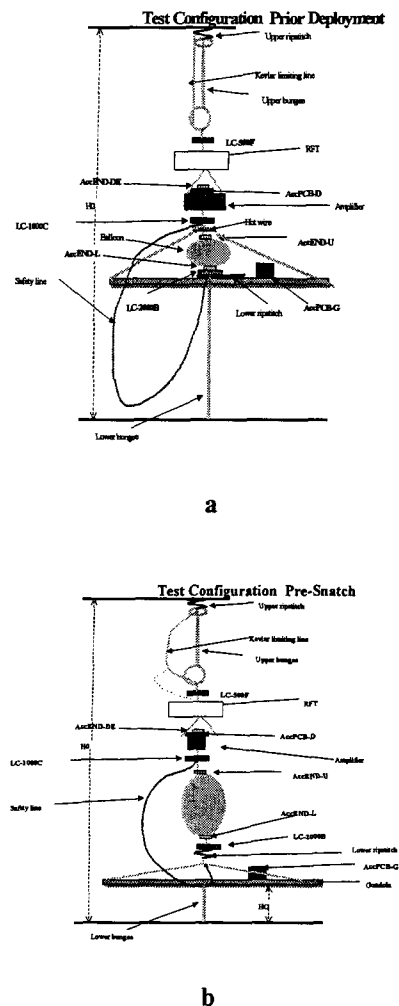
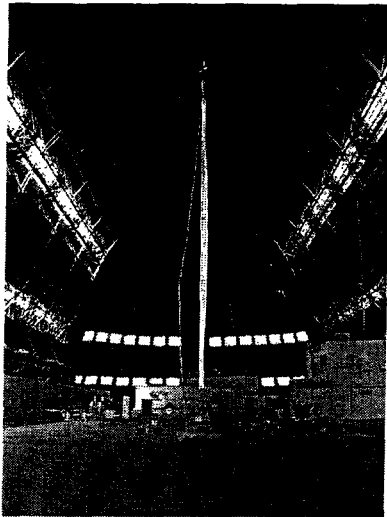


Figure 9. ARC test configuration
a - before deployment, b - after deployment

The 10-m 12m spherical Mylar balloon was packed in our standard "fold-and-roll" method, placed into the Styrofoam container that was suspended on set of 2-4 bungees made of latex tubing. Initial extension of bungees was limited with the parallel Kevlar tether. Ripstitch or another set of bungees used as shock absorber. A 25-kg payload, that simulated inflation module of stratospheric tests, was attached via lower ripstitch to the lower fitting of balloon.

A set of sensors with high-speed registration (5000 samples per second) recorded data during deployment. The set included high-frequency accelerometers on both fittings, load cells in line with both fittings, accelerometers on the payload and on the 2.5 kg unit above upper fitting, a load cell between this unit and the bungee.

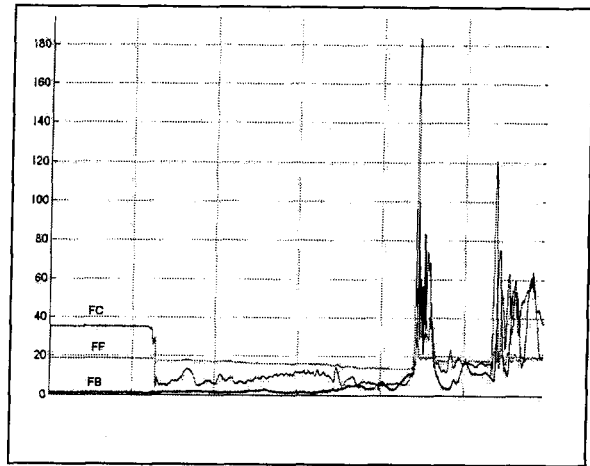
When balloon container opens by remote command the upper part is pulling up by the upper bungee that simulates action of parachute whereas payload either falls free or accelerating further with a lower bungee to increase separation velocity. General view of the test is shown in Figure 10.



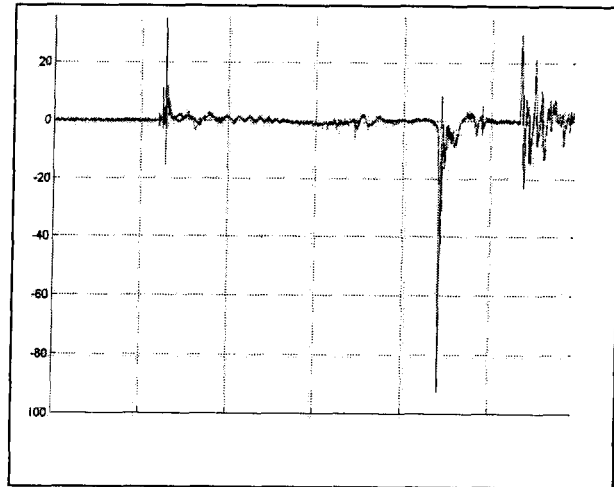
Test B1

Figure 10. General view of deployment tests in Ames hangar

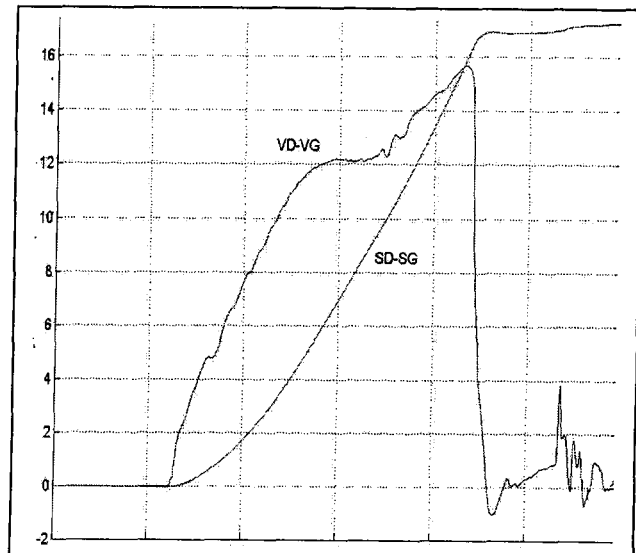
Figure 11 shows examples of data recorded during one of the tests.



a



b



c

Figure 11. Example of recorded data.
a- forces, b - acceleration, c- separation velocity

Fig.11a and Fig.11b show forces and accelerations, Fig.11c – velocity difference between top and bottom of the balloon calculated by direct integration of the accelerometer measurements. The nomenclature is: FB – load cell between the lower fitting and lower ripstitch, FC – load cell between the upper fitting and upper instrument unit (UIU), FF – load cell attached to the bungee above UIU. Accelerometers aG – on the gondola, aL – on the lower fitting, aU – on the upper fitting, aD and aDE – on the UIU. Accelerometers aD and aG had range 0-250 g, aL and aU 0-2000 g. On the timescale distance between the gridlines is 0.5 s.

As seen in Fig.11a, before the balloon container opens, force FC is equal to total weight of suspended module, force FF – elastic force of the extended bungee (part of weight is taken by the limiting Kevlar line) and force FB is negligible since the balloon is at rest within container.

Force FC drops below tension of the bungee when the container opens due to acceleration of non-negligible mass of the UIU (plus cables running signals to the computer). Bungee force FF gradually decreases while bungee is contacting. Interestingly, force FB on lower fitting remains small till the end of the deployment indicating that the lower part of the balloon and the payload fall almost free with very small interaction between them.

At snatch, force applied to the balloon fitting peaks to 180 dN (~180 kG) while force at the bottom fitting is limited with the maximum force of the lower ripstitch. Following high-frequency variations in force FB indicate tearing of the lower ripstitch. After snatch the balloon starts to move down extending bungees and the next peak of both forces FC and FB occurs when the limiting Kevlar line deploys for full length. At this moment the upper ripstitch begins to tear that corresponds to higher-frequency variations in the both forces.

As seen from Fig.11c, at this particular test (test C) velocity at snatch (difference between velocity of the moving up upper fitting and moving down payload and load fitting) was 15.1 m/s. This value is smaller than the static deployment value 17.3 m/s while deployment time was 1.58 s – shorter than at static deployment (1.77 s). It is important to note that

the velocity values derived from one-axis accelerometer measurements in fact represent a minimum estimate of velocity because of possible (and observed) tilt of the accelerometers. It is seen the most clearly in comparing velocities from integrated data of accelerometers aG and aL – giving VG consistently higher values (accelerometer aG was installed on the relatively stable payload while aL – on the least stable lower fitting).

Altogether the same balloon was deployed seven times without failure in spite of repacking and handling. Minimum deployment time 0.87 s (test D3) – significantly shorter than was observed in three stratospheric tests (~1.5 s) while separation velocity was 28 m/s – significantly more than expected value in the stratospheric tests (20-22 m/s).

Peak acceleration of the upper fitting at snatch was ~400 g and lower fitting ~250 g. peak force applied to the top fitting was 312 dN; peak force at lower fitting was limited with the ripstitch and did not exceed 142 dN. Rough estimates of the internal balloon forces gave peak values ~400 dN for the upper fitting and ~200 dN for the lower.

The balloon finally failed at the last test when it was packed in accordion though test setting was relatively benign – separation velocity was only 18.8 m/s. The failure occurred near the boundary between balloon doubler – location where the simulation predicts maximum stresses and where failed balloon at the stratospheric test STRA-4. It is still unclear – was accordion folding responsible for the failure or it effect of the weariness of film or of an undetected flaw developed in previous tests. SEM analysis suggested that the tear could be initiated at a pinhole. The pinhole should be located in the region where internal balloon stress exceeds approximately 0.5 of tensile strength of Mylar (this number was determined from special tests of Mylar film with pinholes). Later deployment test with a pinhole did not result in balloon failure.

Exceeding all expectations robustness of the balloon convinced us that the deployment stresses by itself was not the main reason of the balloon failure in the test STRA-5 and there is no need in development more complicated and hence less reliable deployment schemes.

ADDITIONAL TESTS

A quite comprehensive set of additional tests were conducted on the Mylar balloons and critical elements of the flight train.

Static pull tests when balloon is subjected to 200 dN extension force became regular procedure of quality control during balloon fabrication at GSSL. To measure static deflection characteristics one balloon was stressed to 300 dN without damage.

Vacuum chamber tests intended to estimate force produced by balloon on balloon container during standard procedure of residual gas evacuation. Another goal was to check that the procedure does not damage the balloon. Pinhole detection with helium sniffer in the areas near balloon doubler before and after the vacuum chamber did not find any. Measured forces on the balloon container wall were 1-2 dN and proved to be non hazardous to the balloon.

Storage test was not intentional – we used balloon built in August 2000 i.e. 18 months earlier. During all this time the balloon was stored densely packed in the standard “fold-and-roll” mode. No pinholes or other visible damages were detected. This balloon later passed successfully static deployment test and was successfully deployed in the stratospheric test proving that Mylar balloon can undergo required 9-12 months of storage during tests and interplanetary cruise to Mars.

Tests for deployment-induced defects were performed on four Mylar balloons. As earlier, only areas about 0.3-0.5 m width around boundary of upper and lower doublers were searched - areas which experience most stress concentration and where three failures were observed (two – in flight tests, one – in deployment test). Several small holes were found in two balloons before deployment tests. They were repaired with tape on one balloon but left unrepaired on another. All four balloons passed static deployment tests without failure including the balloon with pinholes. No new pinholes or other defects were detected in the balloons after deployment tests. Though other areas of the balloon were not checked (we did not have resources for such a lengthy procedure), likelihood of deployment-induced defects there seems much less since significantly lower stress in these areas.

Tests on Mylar film demonstrated that *strain-rate effect* was could not be the factor of balloons failure – deployment rates are still well below region where strain rate significantly decreases Mylar strength.

Tests of the ripstitch - another critical element of the flight train did not show any noticeable difference in performance the ripping force at room temperature and at -60C thus excluding possibility being a critical failure factor.

On the other hand, *thermal simulation with a real flight profile* showed that use the fabric bag as balloon container could result in heating of the balloon up to 100-110C during float after ascent. At these temperatures Mylar loses over 50% of its strength that may result in the deployment failure. The fact the STRA-5 balloon failed near the upper doubler was strong indication of this effect.

STRATOSPHERIC TESTS STRA-6- STRA-8

Flight train configuration. Four 10-m spherical 12 μ Mylar balloons and one pumpkin shape 500 m³ polyethylene balloon (see below) were prepared for the next round of stratospheric flight tests.

A number of modifications have been made to the flight train:

- Styrofoam box used as balloon container to insulate the balloon during ascent and float and to eliminate effect of balloon overheating (as well as of cooling of the balloon in cold tropical tropopause).
- The 1kg Upper Instrument Unit (UIU) was included to get data on acceleration and velocity of upper part of the balloon during deployment and to measure temperature of the top fitting during ascent and float.
- Two additional ripstitches were installed – one between the UIU and upper fitting, another between the upper TV-unit and parachute. Purpose of the first one was to limit force applied to the balloon at snatch when the UIU has to be accelerated with 100-200g. The other ripstitch (8-m long when torn) was installed to increase distance between balloon and parachute after deployment and reduce wake effect of the inflated balloon on the parachute. Rip force and length of the ripstitches were selected

by results of stratospheric deployment simulation.

- The flight computer and software were simplified to improve reliability and shorten time of integration and tests.
- An independent device to send commands for deployment and inflation used as back-up.
- Two pyro guillotines were excluded – one to release parachute, another – to release inflation system with a purpose to simplify system and to make possible recovery of the flight train.
- Two cameras previously used in other stratospheric tests were installed to improve quality of imaging (it turned out to be a bad decision and the former cameras were re-installed after the first test).

Pumpkin balloon.

In addition to spherical superpressure balloons, pumpkin shaped superpressure balloons have been flown at Earth for extended durations. Since 1998, NASA's Balloon Program Office at Goddard Space Flight Center's Wallops Flight Facility has been developing an Ultra Long Duration Balloon (ULDB) capability for payloads up to 2800 kg utilizing the lobed pumpkin balloon design. The ULDB technologies have been employed in the construction of prototype pumpkin balloons for Mars.

Two 500 m³ pumpkin shaped balloons were manufactured by Raven Industries as part of the NASA Cross-Enterprise Technology Development Program. Two different thicknesses of linear low density polyethylene (PE) film were used: 20 μ (0.8 mil) and 8.9 μ (0.35 mil). The load tendons on both balloons were constructed from poly(p-phenylene-2,6-benzobisoxazole) (PBO) braided fibers. When inflated, these balloons have a diameter of 11.34 m and a height of 6.8 m.

The choice of PE film was validated by laboratory testing. Even though the cold brittleness (CB) temperature when determined dynamically with the ball drop test for PE is approximately -95 C, cylinder pressure tests of PE at -130C validated that the material is not brittle when statically loaded [8]. In addition, when intentional holes or cracks were placed in the cylinders, failure did not occur due to initiation of the induced damage. Since, PE has

a higher toughness than Mylar, the risk of damage during the dynamic inflation process is also reduced as long as the film temperature is above -95 at the time. Therefore, PE is a feasible candidate for non-environmentally extreme Mars Balloon mission.

The pumpkin design has several advantages for the Mars Balloon mission. First of all, the high-strength tendons, rather than the film, take the shock loading during the aerial deployment of the balloon. Secondly, in order to accommodate a higher superpressure with the pumpkin design, the bulge radius can be reduced (which increases the number of gores) to maintain the same strength requirement of the film. The spherical design requires a higher strength (and heavier) film to accommodate a higher superpressure.

The 20μ (0.8 mil) balloon was successfully deployed in a hangar drop test at Ames and then successfully deployed and inflated in the stratosphere in June of 2002.

Pre-flight deployment tests. In oppose to prevailing views and our former practice to handle Mylar balloons as less as possible between fabrication and flight tests we decided to conduct hangar deployment tests on all balloons before stratospheric tests. Arguments in favor were successful deployment of the balloon at test STRA-2A – the balloon that was subjected to intensive handling, deployment and inflation tests and was repacked several times. Another argument was that deployment and associated shock loads may find a “birth mortality” defect in the balloon. Third argument was to test the whole flight train in the configuration that later will be used in stratospheric tests following “test as fly” philosophy.

Four Mylar balloons and 20μ pumpkin PE balloon were deployed at the ARC hangar in April 2002 by the method developed previously. The pumpkin balloon was packed in accordion while the Mylar balloons were packed in “fold-and-roll”. The same set of bungees used to simulate stratospheric deployment. New data units developed for stratospheric flight – one installed on the payload, another as the UIU were calibrated using the in parallel the same set of independent sensors as in the October 2001 tests.

All five balloons were deployed successfully. Careful inspection of locations where damage would be most likely – boundary of doubler at

spherical balloons and entries of tendons in the guiding sleeves at pumpkin balloon – did not reveal any deployment-induced damages.

Both data systems produced measurements close to the reference set. Separation velocity at parachute release were 18-20 m/s for spheres and XX m/s for pumpkin balloon, respective deployment times was 1.5 and 1.6 sec.

General description of stratospheric tests STRA6 – STRA8

Three stratospheric flight tests STRA-6, STRA-7 and STRA-8 have been conducted respectively on June 2, June 5 and June 8, 2002. Tests STRA-6 and STRA-8 used spherical Mylar balloons, STRA-7 – pumpkin balloon.

Due to undetected error in commercial software of telemetry system, telemetry data from the tests STRA-6 and STRA-7 were received only to approximately 50 km distance. After test STRA-7 this error has been corrected and data from the test STRA-8 were received during all flight until the ocean touchdown. Radiosonde measurements were received during whole durations of all three tests.

Both cameras and TV-link provided continuous coverage of all three tests from launch to landing. Not a single TV frame was lost during deployment and inflation of the balloon. Though transmitted in analog form, TV-images were recorded in digital format for subsequent frame-by-frame analysis. Being very clear during float, images of the DM and balloon from the down-looking camera at test STRA-7 became glared after parachute release. Process of balloon inflation is visible only in video when eye will integrate and filter balloon image. Change of cameras on the other flights fixed this problem.

Cruciform parachute with anti-inversion mesh of 10.8 m (36') size used in tests STRA-6 and STRA-7, larger 13.8 m (46') cruciform parachute without mesh used in STRA-8.

Results of tests

All three tests followed the same scenario. Data from radiosondes, GPS and cameras in combination with log-file of the master ground computer used to reconstruct time and altitude history of each test. Main events of the tests are shown in Table 2.

Table 2. Main events of stratospheric tests STRA6-STRAS

	STRA-6		STRA-7		STRA-8	
	time,s	h,km	time,s	h,km	time,s	h,km
Launch	-6132	0.58	-6218	0.58	-5137	0.58
Parachute for release	0	34.6	0	34.1	0	34.5
Balloon deployment	46.4	33.2	36.4	32.9	44.2	33.3
Inflation-1	89.5	31.7	68.0	31.7	65.6	31.7
Inflation-2	117.4	30.8	91.6	31.0	117.3	23.3
Balloon failure	144	30.0	none	none	46.0	33.2
DM landing	4579	0	4005	0	637	0

Ascent to float altitude took 86-88 min. Float altitudes correlate with mass of the system: STRA-6 flight train was the lightest, that of STRA-7 was heaviest and respective float altitude were the highest and lowest ones.

Characteristically, all three balloons were deployed almost at the same altitude – at approximately 33 km and inflation began at altitude 31.7 km (ambient pressure 9.5 mbar). Densities at these levels – 11.6 and 14.0 kg/m³ correspond respectively to altitudes 2.5 km and 0.75 km in the Southern hemisphere of Mars in the middle season.

Test STRA-6

Pressure and temperature measurements by radiosonde gave estimates of descend velocity and dynamic pressure during deployment and inflation process as shown in Fig. 12.

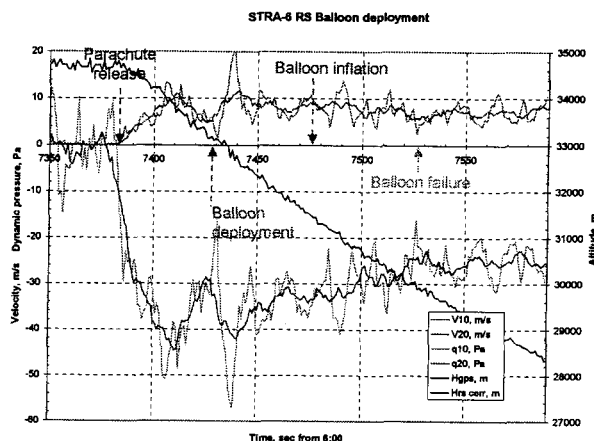


Figure 12. Velocity and dynamic pressure during STRA-6 deployment and inflation process

The plotted are velocity and dynamic pressure from linear least-square estimates on intervals 10 and 20 s. Accuracy of the radiosonde measurements is insufficient for detailed analysis but the parachute release is seen easily. The most likely values of descent velocity and dynamic pressure at the moment of balloon deployment were close to 38 m/s and 8 Pa respectively.

Clear images from the up-looking camera gave unambiguous evidence of successful balloon deployment. Some of them are shown in Fig.13. Fig.13a shows image before deployment with the parachute and parts of balloon container in field of view. Fig.13b shows intermediate phase when balloon is in process of deployment and Fig.13c – view of deployed Mylar balloon with parachute two seconds after deployment.

As far as it can be judged from the video, no major instabilities were observed during balloon inflation; balloon motion resembled motion of a jellyfish. There is no evidence of abrupt flagging motions that could be really hazardous to balloon film. Observed motions of balloon envelope reflect also lack of pressure of helium within the balloon since 400 g of gas in tank could to fill only 40-50% of balloon volume at altitudes of inflation. Images in Fig.14 (at the end of the paper) show balloon during inflation process with interval 10 seconds.

The balloon failed 54 sec after start of inflation. As can be judged from up-looking camera images, The failure occurred somewhere in the upper part of the balloon. In several seconds of descent the balloon was destroyed but the inflation windsock that was attached with ribbon to the upper fitting remained intact and the flight train consisting now of the parachute with suspended deployment /inflation module and other components continued descent and landed in ocean 75 minutes later.

We'll discuss possible failure modes after description of the next test STRA-7 where clear pictures from both cameras revealed new details about behavior during inflation process.

Test STRA-7

By the moment of balloon deployment descent velocity and dynamic pressure were 39 m/s and 8.1 Pa - approximately the same as for previous flight. The balloon, folded in accordion, was deployed successfully. Fig.15 shows pictures at one moment during balloon deployment made from both – up-looking and down-looking cameras.

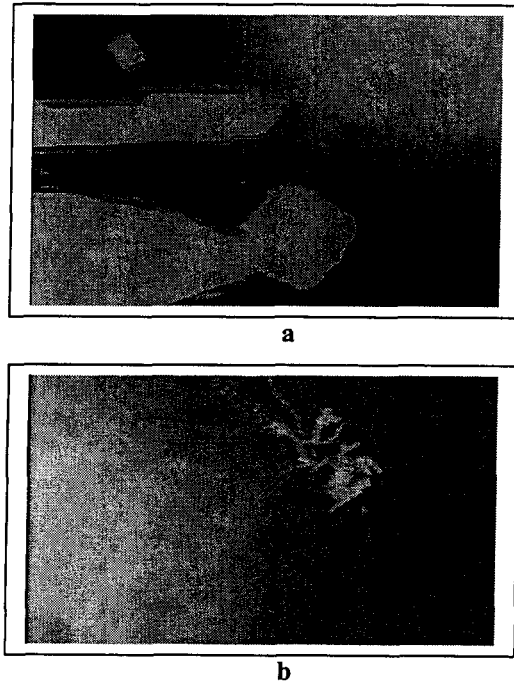


Figure 15. Pumpkin balloon 0.57 s after beginning of deployment

a-up-looking camera, b-down-looking camera
 Shortly after beginning of inflation tension in the link connecting the upper camera unit with the upper balloon fitting dropped significantly and the line became almost loose (this link was consisted of ripstitch, the UIU and Kevlar tethers). It was result of larger diameter and drag of the pumpkin balloon. As a consequence, the balloon with suspended DIM and parachute descended for a while in parallel being connected with unloaded link between them. This provided an opportunity to received unique side-view pictures of the balloon that unlikely will be obtained in future.

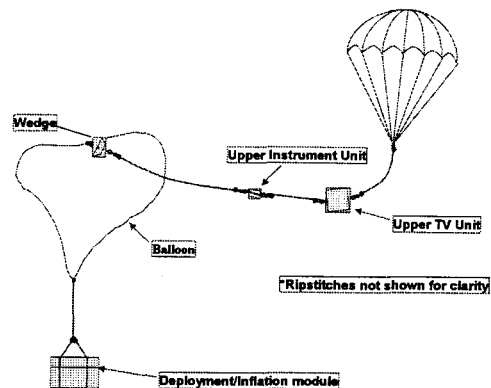


Figure 16 shows geometry of viewing at this phase. At some phases balloon could be even above higher than the down-looking camera.

Figure 16. Geometry of down-looking camera viewing during balloon inflation

Lack of tension in the link lead to chaotic motions of camera – both in translation and in rotation with balloon (and Earth at the background) violently moving around and sometimes disappearing from the field of view of camera.

One of the most spectacular pictures (Fig. 17) shows descending balloon with the clear boundary of the troposphere, curvature of the Earth and Big Island of Hawaii at the background.

In subsequent frame-by-frame analysis of the period of first two minutes after start of inflation, we used details on background (Earth, clouds, Sun) and balloon itself to decrease effect of rotation of the camera by counter-rotation of images.

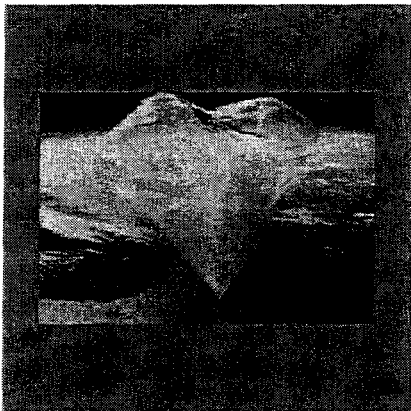


Figure 17. Balloon after 91.6 sec of inflation (Big Island of Hawaii at left)

Up-looking camera images showed slower rotation and oscillations of the DIM.

The parachute and the Sun reflection on camera walls were used as reference for counter-rotation

of the up-looking camera images. **Fig.18** (at the end of the paper) shows a gallery of synchronous pictures from the both cameras with intervals approximately 10 s.

The most important features of the balloon behavior under inflation are:

- Shortly after beginning of inflation the balloon took a spoon-like spinnaker shape with the DIM at the bottom. It could be result of wind shear or side drag by the parachute or both;
- Most of the time balloon preserves a “mushroom” though asymmetrical shape
- Bottom suspension of the DIM ensured, as in the test STRA-6, descent without major instabilities;
- Loose link between the down-looking camera unit and the balloon upper fitting made imminent the UIU that was only about 1 m from the balloon touched and actually laid on the balloon film itself many times. The 20 μ polyethylene that the pumpkin balloon was made of was robust enough not to be damaged by this. However if this did happened with the Mylar balloon it would be destroyed almost instantly.

Actually it could be one of the most likely reasons of the observed balloon failure in the test STRA-6 where the UIU that had relatively sharp corners was at the same 1 m nominal distance from the balloon. Wearing of the balloon material with motions during descent could be another factor.

Later in descent the balloon contracted with increase of ambient pressure, its drag decreased and the balloon returned to its position under the parachute. The whole flight train landed in the ocean 1h 7 min after release from tow-balloon. The flight train was recovered shortly after landing. All components, especially the balloon were inspected. Unfortunately, during recovery the balloon was severely damaged with the boat propeller that essentially destroyed all lower part of the balloon. Measurements of turn lengths of the ripstitches will be used to improve model of the deployment simulation.

Test STRA-8

In this test we used larger parachute and took other precautions to prevent possibility of balloon damage. The Upper Instrument Unit was placed above the down-looking camera unit, an

additional 3-m Kevlar tether was installed between main ripstitch and the upper fitting, all components were wrapped with a soft material. As result no hard surface were closer than 5 m to the balloon during ascent and expected to be not closer than 9 m when the ripstitch would tear after balloon deployment.

Due to the larger parachute the descent velocity and dynamic pressure were significantly lower – 32 m/s and 5.3 Pa.

As witnessed by video, shortly after the parachute release the destruct line and torn gore (50-m long) of the carrier balloon fell down and tangled around elements of the flight train and most importantly – around the main ripstitch thus preventing it from normal performance.

Without shock absorption the subsequent balloon deployment was destined to fail and the balloon was ruptured somewhere in the upper part.

The DIM separated and started to fall free; in 10 min it reached the ocean. Video was received during all the way during fall in spite of a quite violent motion of the DIM. The parachute with down-looking camera continued to descend and “landed” in the ocean 2 hrs 10 min later.

The helium tank was discharged during the fall by the ground commands. Measurements of the acceleration of the DIM, tank pressure and temperatures of the inflation system components were received via the telemetry system. Acceleration data showed that the balloon deployment took 1.50 s and the lower ripstitch was torn for 55 msec before the balloon failure. Measurements of tank pressure and temperatures allowed to improve model of operation of the inflation system.

Further steps

There are several areas that need further adjustment. The results of the tests shows that shortening time of inflation would be beneficial – it will decrease time when balloon material is loose and exposed to wearing, it will lighten requirements for entry and deployment performance since inflation can be done over shorter altitude range.

At least in case of the pumpkin balloon the parachute should be released 10-20 sec after beginning of inflation. For the spherical balloon larger parachute should be used.

Additional simulation of the inflation system needed to optimize it parameters. Aerodynamic simulation of the aerial inflation will help system design.

Most likely 2-3 stratospheric tests would be required to complete the technology validation.

CONCLUSIONS

Success of the current phase of the Mars Balloon Validation Program provided solid base for commitment to Mars balloon mission.

The main accomplishments are:

- Developed and successfully validated technology of aerial deployment of light-film balloons in the atmospheres of Venus and Titan (it was a by-product of the Mars balloon technology development).
- Developed and successfully validated the technology of aerial deployment of full-scale light-film balloons in the most challenging Mars-like environment. It has to be mentioned that balloon deployment at the Earth stratosphere is even more stressful than deployment on Mars due to significantly higher value of acceleration of gravity that controls accelerations and deployment forces. It ensures even bigger margins for deployment in the Martian atmosphere.
- Validated technology of inflation of polyethylene pumpkin balloon
- Conducted comprehensive test program encompassing majority of features of Mars balloon mission
- Proven viability of two balloon types – spherical Mylar and polyethylene pumpkin – for Martian application
- Developed prototypes of inflation and deployment systems that can be used for the Mars mission.
- Developed procedures and logistics for low-cost year-round stratospheric tests;

The MABVAP accomplishments laid the foundations of two recent Mars Balloon mission proposals: Piccard Discovery and Piccard Mars Scout. We are convinced now that the technology is proven to be mature enough to be selected for the Mars mission

Acknowledgements:

The research described in this paper, was carried out by Jet Propulsion Laboratory, California Institute of Technology, under a contract with National Aeronautics and Space Administration with collaboration of Balloon Program Office of Wallops Flight Facility NASA Goddard Space Flight Center. Contributions from the other members of MABVAP team are greatly acknowledged.

References

1.A.Vargas, J.Evrard, P.Maurois. Mars 96 Aerostat. – An Overview of Technology Developments and Testing. AIAA International Balloon Technology Conference, San-Francisco, CA, 1997

2.R.Zubrin, S.Price, B.Clark, J.Cantrell, R.Burke. A New MAP for Mars. Aerospace America, September 1993, p.20

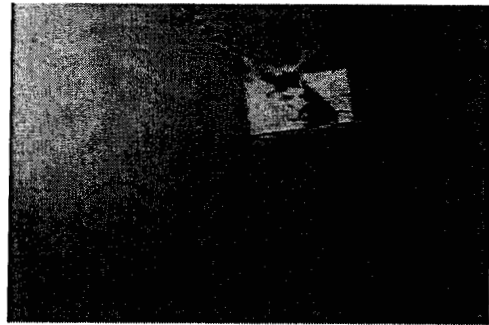
3.Mars 2001 Aerobot/Balloon Study (MABS). JPL Internal Document, 1996

4. V.Kerzhanovich, J.Cutts, A.Bachelder, J.Cameron, J.Hall¹, J.Patzold, M.Quadrelli, A.Yavrouian, J.Cantrell, T.Lachenmeier, M.Smith.Mars Aerobot Validation Program. Paper presented to AIAA Balloon Technology Conference. Norfolk, VA, June 1999

5.J.Cutts, V.Kerzhanovich, J.Jones. Balloons for Planetary Exploration. Paper presented to 2000 COSPAR Meeting, Warsaw, Poland.

6. H.M. Cathey, Jr., M. Smith and R. Stephens. Design and Testing of the ULDB Vehicle, COSPAR, Warsaw, Poland, 2000

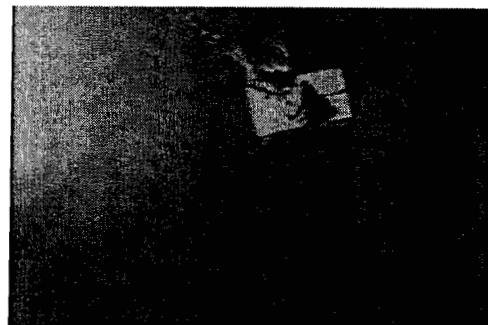
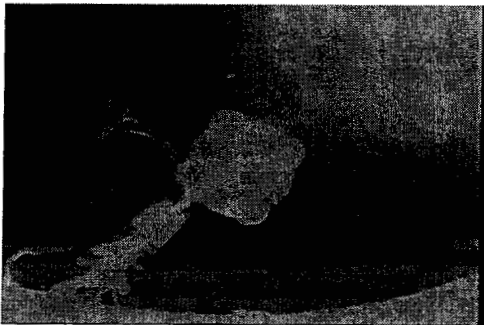
7. M.Said. Preliminary Study on Polyethylene for Consideration as a Structural Envelope Material for Mars Balloons. WFF Memo MAS 071801-001, 2001



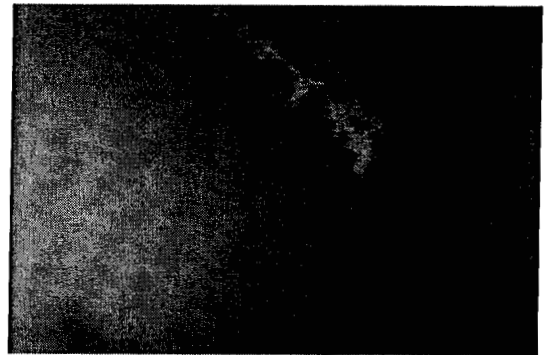
Cam-1 #230 T=0.100 s Cam-2 #174



Cam-1#231 T=0.133 s Cam-2 #175



Cam-1#232 T=0.167 s Cam-2 #176



Cam-1 #251 T=0.800 s Cam-2 #195



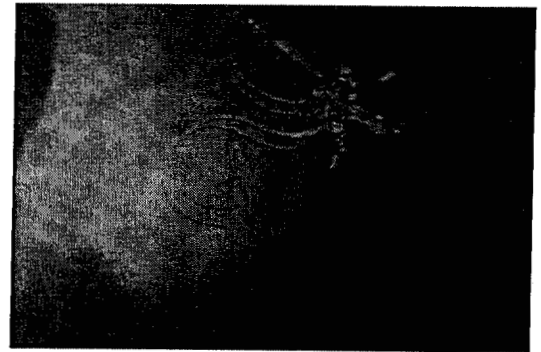
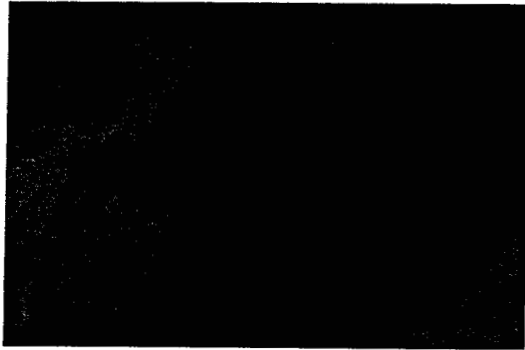
Cam-1 #252 T=0.833 s Cam-2 #196



Cam-1 #253 T=0.867 s Cam-2 #197



T=1.800 s



T=1.833 s



Cam-1 #280 T=1.867 s Cam-2 #227

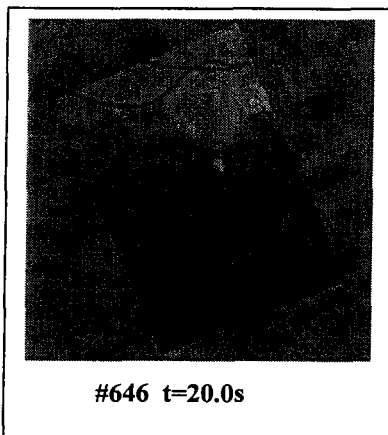
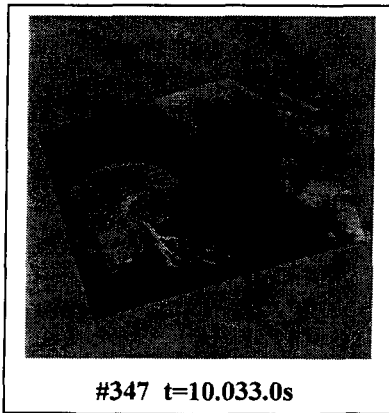
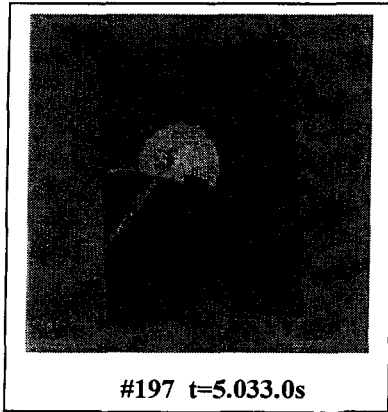
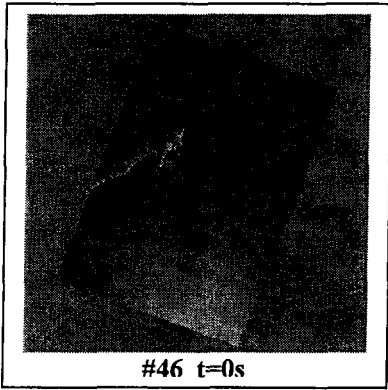
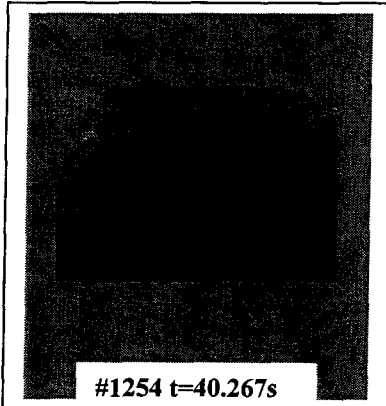


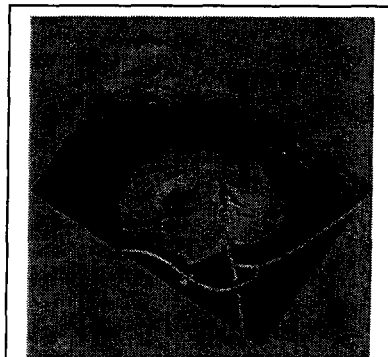
Figure 18.1-18.4. Test STRA-7.Pumpkin balloon during inflation



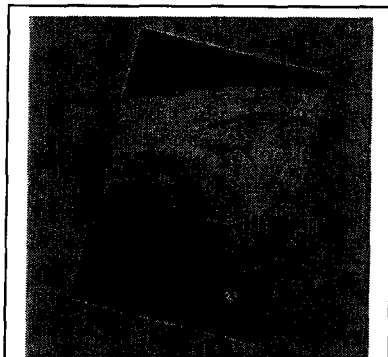
#959 t=30.433.0s



#1254 t=40.267s



#1545 t=49.967s



#1849 t=60.100s

Figure 18.5-18.8. Test STRA-7.Pumpkin balloon during inflation (continue)

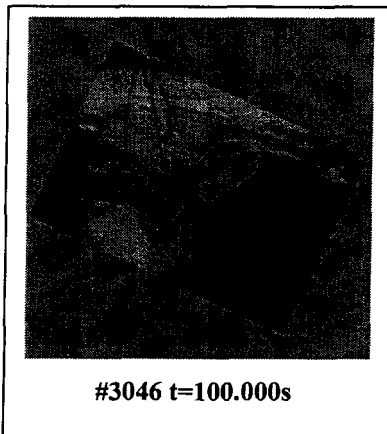
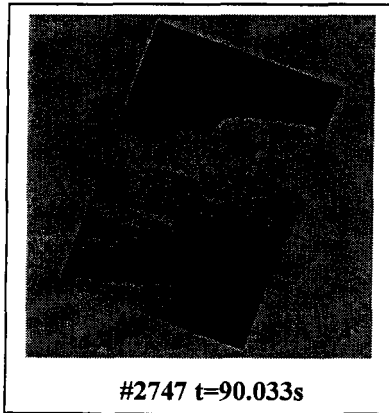
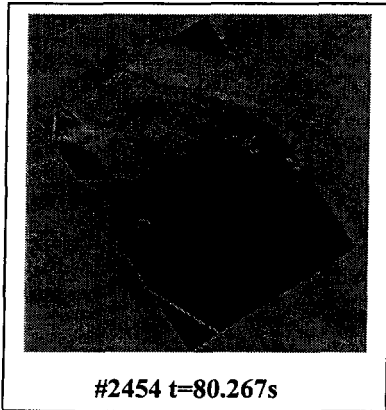
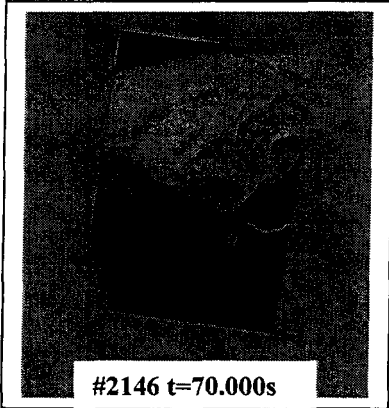


Figure 18.9-18.12. Test STRA-7.Pumpkin balloon during inflation